Chirality correlation in double-wall carbon nanotubes as studied by electron diffraction

Kaori Hirahara,[1,*] Mathieu Kociak,[2] Shunji Bandow,[1] Takanori Nakahira,[3] Kouji Itoh,[3] Yahachi Saito,[3,4] and Sumio Iijima[1,5]
[1]*Department of Materials Science & Engineering, 21st Century COE, Meijo University, 1-501 Shiogamaguchi, Tenpaku-ku, Nagoya 468-8502, Japan*
[2]*Laboratoire de Physique des Solides, bâtiment 510, Université Paris-Sud/ CNRS UMR8502, F-91405 Orsay, France*
[3]*Department of Electrical and Electronic Engineering, Mie University, 1515 Kamihama, Tsu, Mie 514-8507, Japan*
[4]*Department of Quantum Engineering, Nagoya University, Furo-cho, Chikusa-ku, Nagoya 464-8603, Japan*
[5]*NEC Corporation, 34 Miyukigaoka, Tukuba 305-8501, Japan*
(Received 27 September 2005; revised manuscript received 22 February 2006; published 23 May 2006)

Structural correlation between two adjacent graphitic layers in double-wall carbon nanotubes (DWNTs) was systematically examined by using electron diffraction. Chiral angles and tube diameters were carefully measured, and the chiral indices of individual DWNTs were accurately determined. As a result, it was found that the interlayer distances of DWNTs were widely distributed in the range between 0.34 and 0.38 nm. Chiralities of the inner and outer tubes tended to be distributed at higher chiral angles, approaching 30°, for the tubes with diameter $D<\sim 3$ nm. On the other hand, for the tubes with $D>\sim 3$ nm, the chiral angles were widely distributed, covering the chiral map entirely. Therefore, we consider that tubes with small diameters have a tendency to form armchair type. Correlation of chiralities between the inner and outer tubes was found to be random.

DOI: 10.1103/PhysRevB.73.195420 PACS number(s): 61.46.−w, 61.14.Lj, 81.07.De, 61.48.+c

I. INTRODUCTION

It has been suggested that multiwall carbon nanotubes (MWNTs) grow by the layer-by-layer growth mechanism.[1,2] It is of interest to know if there is any directional correlation between two adjacent graphitic layers in a MWNT when it grows. An experimental study on the structural characterization of MWNTs suggested that graphitic layers in a MWNT exhibit a variety of chiral angles.[3] Electron diffraction (ED) is a quite useful method for examining the chiralities of not only the top layer, but also all the other layers constituting a single MWNT, because the pattern of a MWNT can be explained as the sum of the individual diffraction patterns of all the nested single-wall carbon nanotubes (SWNTs).[3–7] Therefore, structural correlations between two adjacent layers can be examined experimentally. The correlations have been discussed theoretically in terms of the commensurability of two adjacent layers in a MWNT.[8,9]

It is noted that the ED pattern for a single MWNT is rather complicated, so that generally it is not practical to examine the MWNT for the present purpose. Therefore, we choose an extreme case of a MWNT, a double-wall carbon nanotube (DWNT) consisting of only two layers. In this case, its structural characterization becomes much easier than for the MWNT, and thus correlations between the layers of inner and outer tubes can be studied in detail.

II. EXPERIMENT

A. Preparation of DWNTs

The DWNTs used in the present experiment were prepared by the arc discharge method. A pure carbon rod 10 mm in diameter was employed for the cathode, and a carbon rod 5 mm in diameter, which has a cylindrical hole 4 mm in diameter and ~15 mm in depth at the center of the rod tip, was used for the anode. The hole was filled with a mixture of carbon powder and metal powders with the ratio Fe:Ni:Co:S:C=5:5:5:10:75 (wt %). The arc discharge operation, which was carried out using an electric current of 50 A in hydrogen gas at 300 Torr at room temperature, allows selective formation of the DWNTs. They were found in the soot deposited on the inner wall of the chamber as well as at the bottom portion of the cathode. The products, collected from the inner wall of the chamber, were sonicated in *n*-hexane by using a conventional ultrasonic bath in order to prepare a sample for electron microscopy. The colloidal suspension thus prepared was collected onto standard grids for high-resolution transmission electron microscope (HRTEM) observation, which allows us to easily select an isolated nanotube present in the specimen.

B. HRTEM observation

We selected an isolated DWNT dispersed on the specimen grid, and recorded the HRTEM image and ED patterns from the same region of the DWNT. HRTEM observations of DWNTs were carefully carried out in order to reduce electron irradiation damage. A HRTEM (a JEOL JEM-2010F) of a spatial resolution of ca. 0.14 nm was operated at an acceleration voltage of 120 kV, which is below the knock-on damage threshold of 140 kV for graphite. The dose of the electron beam was kept as low as possible for transmission electron microscope (TEM) observation, and was 4.2×10^5 electrons/nm^2 (0.013 pA/nm^2 for 2 s) for HRTEM imaging and $1.3\times 10^7-3.2\times 10^6$ electrons/nm^2 (0.20–0.05 pA/nm^2 for 4 s) for ED recording. Electron irradiation damage to the DWNTs during recording ED patterns was monitored by inspection of HRTEM images, where any damage was detected before and after recording the ED patterns. It was confirmed that no appreciable tube damage occurred under the present experimental conditions even with 1 min exposure time.

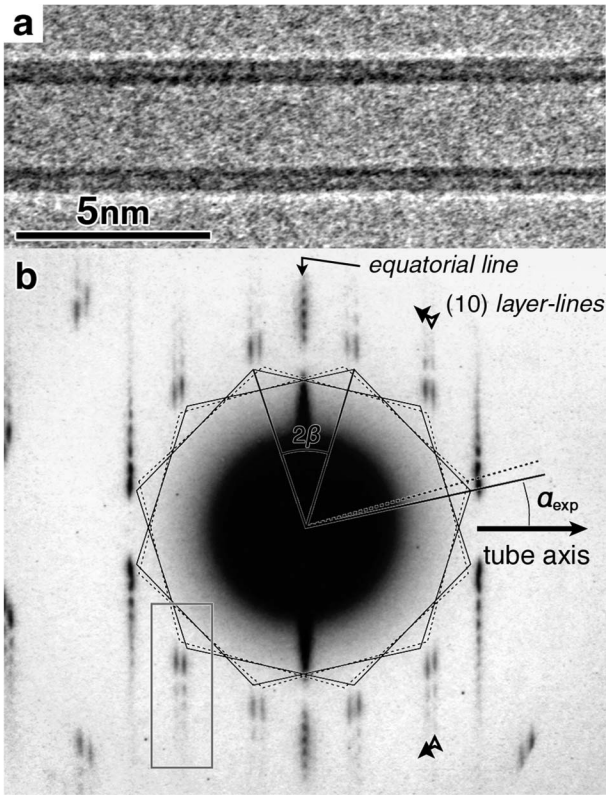

FIG. 1. (a) HRTEM image and (b) corresponding ED pattern of a DWNT, for which the chiral indices are determined as $(28,11)@(37,11)$.

Furthermore, it is noted for recording ED patterns from a single nanotube that we used a small condenser aperture 10 μm in diameter for selecting the irradiation area (<10 nm) instead of using the convergent electron beam. Here we tuned the electron beam in the $\alpha 1$ mode for JEM-2010F; this mode is generally used for HRTEM imaging with a magnification greater than 200 000 times. The rather "parallel" beam obtained thus allows us to record the sharp features on the diffraction spots, although the conventional nanobeam electron diffraction method with a convergent beam leads to a diffused feature on the diffraction spots and reduces the resolution of the ED patterns. This mode of operation is called "nanoarea diffraction,"[10] and is more usually known as "Koehler illumination" (see the illustration in Ref. 11).

C. Structural characterization of a DWNT by electron diffraction

The atomic structure of a carbon nanotube is defined by a pair of integers (n,m), called the "chiral index." An ED pattern taken from a single nanotube provides values for two structural parameters of the nanotube: the chiral angle (α) and the diameter (D). These two parameters have relationships with the chiral index, which are given by

$$\tan \alpha = \frac{\sqrt{3}m}{2n+m} \tag{1}$$

and

$$D = \frac{a_{\text{C-C}}}{\pi}\sqrt{3(n^2+nm+m^2)}. \tag{2}$$

Here, $a_{\text{C-C}}$ is the carbon-carbon bond length for nanotubes and equal to 0.144 nm,[12] and α is in the range of $-30° < \alpha \leq 30°$. Both α and D can be determined simultaneously by analyzing an ED pattern of a singe nanotube. Therefore it is possible to determine directly a pair of chiral indices for the inner and outer tubes of a single DWNT. We designate the pair of chiral indices of a DWNT as $(n_i,m_i)@(n_o,m_o)$, where (n_i,m_i) and (n_o,m_o) are chiral indices for inner and outer tubes composing the DWNT.

In the following, we describe a procedure for determining the chiral indices of a DWNT by examining the ED pattern. As a supporting example through the following description, we present a HRTEM image and its corresponding ED pattern of a DWNT in Figs. 1(a) and 1(b), respectively. In order to explain the detailed features of the ED pattern for a DWNT, we will first explain a typical ED pattern of a single SWNT. The diffraction intensities of a SWNT are represented by a set of diffraction lines perpendicular to the tube axis (called the "layer lines"[13]), due to discrete translation invariance along the tube axis. The diffraction intensity along a layer line becomes diffuse and oscillates due to the finite width of the diffracting nanotube. The latter pseudo-oscillation periods are directly linked to the diameter of the nanotube. Furthermore, the first maxima of each line are reminiscent of the (hk)-type diffraction spots for a graphene sheet.[14] It was early recognized that the rotational angle of the line passing by the diffraction center and these maxima with respect to the tube axis [see Fig. 1(b)] are closely related to the helicity.[3]

Accordingly, both helicity and diameter of a SWNT can be examined from its ED pattern. If both the inner and outer tubes of a DWNT have layer lines at nonoverlapping positions, which is the case for incommensurate tubes, the layer lines can be analyzed in the same way as proposed for SWNTs,[5,6] except for the central layer (called the "equatorial line"), in which the diffraction amplitudes of the two tubes interfere with each other.[15–18] The diameters of the two tubes can still be deduced either from the nonequatorial lines, in the easy cases, or from the equatorial line.

The procedure to determine the chiral indices $(n_i,m_i)@(n_o,m_o)$ in the present experiment is summarized briefly as a flowchart appeared in Fig. 2. In the following sections, details of the refinement procedure shown in Fig. 2 are explained by using the ED pattern shown in Fig. 1. First, the measurement of the apparent helicities is described in Sec. II C 1. The problem when the nanotube is tilted against the incident beam direction is discussed in Sec. II C 2. It will be shown how to attribute each layer line in the ED pattern to either the inner or the outer tube of the DWNT (Sec. II C 3). Then, we deal with the measurement of tube diameters (Sec. II C 4), and finally show how to determine the chiral indices with an aid of simulated diffraction pattern (Sec. II C 5).

1. Measurement of apparent chiral angle

The chiral angle of a nanotube can be obtained by examining the locations of layer lines. As stated in earlier papers,

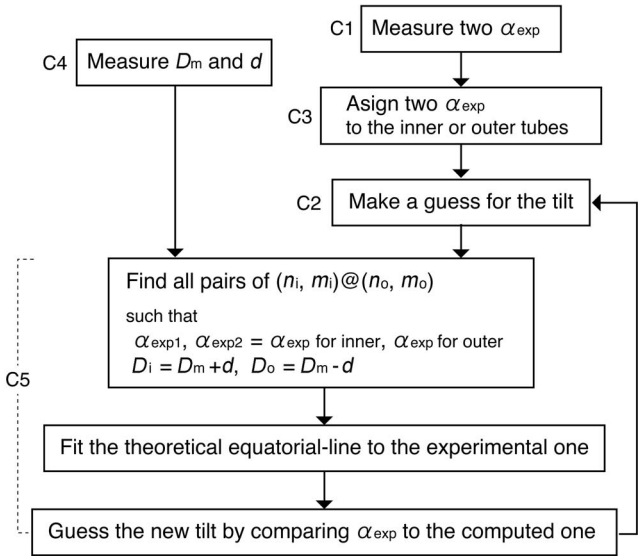

FIG. 2. Procedure to determine chiral indices of a DWNT. The determination of the chiral indices is based on the measurement of apparent chiral angles and diameters can be refined by semiquantitative analysis of the ED pattern. Numbers C1–C5 correspond to Secs. II C 1, II C 2, II C 3, II C 4, and II C 5, where the details are explained.

an ED pattern from a single SWNT shows two sets of layer lines,[6] and the first peak maxima of each set of layer lines indicate sixfold symmetry. The two sets of layer lines have rotation symmetry of π with respect to the tube axis, since they are regarded as the diffraction from two graphene sheets from the top and bottom portions of the SWNT.

Now we consider in terms of a single DWNT. If the inner and outer tubes of the DWNT do not have the same chiral angle, these two tubes should give four sets (two pairs) of hexagonal patterns. Since the inclination of the hexagon to the tube axis is related to the chiral angle α,[6,7] we can measure the chiral angles of the inner and outer tubes of a DWNT. It should be noted that the apparent chiral angle appearing in the ED pattern (α_{exp}) differs slightly from the true value of the chiral angle (α) due to the diffused features of the layer lines in the radial direction of a nanotube. Such a diffuse feature causes a shift of the first peak maxima of layer lines toward the exterior in the radial direction, which leads to a systematic error in the chirality measurement. The systematic error for α_{exp} will be dealt with later. In addition, it is noted that an (n,m) tube with a negative m value is equivalent to an $(n+m,-m)$ tube, which means that the value of α_{exp} is the absolute value of the true one.

In Fig. 1(b), the first peak maxima in the 24 oscillating layer lines correspond to (10)-type diffraction spots, and form two types of hexagons, as shown by the dotted and solid lines. Each hexagon has apparent chiral angles (α_{exp}) for the inner and outer tubes of the DWNT. In order to minimize the measurement error, we actually measured the angle of 2β [see definition of 2β in Fig. 1(b)] instead of α_{exp} where $\beta=30-\alpha_{exp}$. Since the reading error comes mainly from the diffused features of the diffraction rods in the radial direction, measurement of 2β near the equatorial line becomes more accurate.[16] In the case of Fig. 1(b), values of β for the two hexagons indicated by dotted and solid lines were measured as $13.3°\pm0.3°$ and $16.5°\pm0.4°$, respectively. Therefore, α_{exp} for these can be estimated, respectively, as $16.7°\pm0.3°$ and $13.5°\pm0.4°$.

2. Tilt of a nanotube against the incident beam

Most nanotubes observed by HRTEM do not lie perpendicularly to the incident electron beam but slightly tilted. Such a tilt makes the positions of the layer lines shift in the axial direction and the shift causes an error proportional to $1/\cos\theta$, where θ is the tilt angle of the nanotube against the incident plane of the electron beam. This error becomes seriously large in the determination of chiral angles with increasing θ. It is therefore essential to deduce the tilt angle in order to correct the measured values of chiral angles. Here we consider an ellipse passing by the edges of the first peaks of the layer lines, and roughly deduce the value of θ from the aspect ratio of the ellipse. For example, if the tube is exactly normal to the electron beam ($\theta=0°$), the ellipse should be approximately a circle. In case of the ED pattern in Fig. 1, the aspect ratio of the ellipse is estimated to be about 1.03, and the tilt angle is deduced to be less than 5°. As a result, the error of 2β due to the tilt is found to be less than 0.1°, which is very small and practically irrelevant. For the few tubes with large tilt angle, we need to conduct careful analysis by using simulated patterns as shown in Sec. II C 5.

Another elegant method to measure the chiral angles of tilted nanotubes was reported by Gao *et al.*, and is based on the distance ratios between layer lines, and the measurement is consequently independent of the tube inclination.[10] Furthermore, the error on the helicity is very small, because these authors measure the positions of the layer lines in the axial direction in order to minimize the error.[15,17,19] Concerning the measurement of diameters as well as the deduction of the chiral indices from both the diameters and helicities, the method of Gao *et al.* is identical to that employed in the present study. That is, these two methods gave the same results as we have checked for several nanotubes. Although the method reported by Gao *et al.* is rather easier, it requires two or three different layer lines. On the other hand, our method requires only one layer line. This fact works advantageously in practical measurements, since we cannot always see all layer lines of both inner and outer tubes in the observed ED pattern of a DWNT. For example, in the case of nanotubes with large tilt angle, the intensities of the layer lines apart far from the equatorial line have a tendency to decrease. In addition, diffraction intensities from a nanotube with a specific type of chiral structure disappear in accordance with the extinction rule.[17] Therefore, we applied the same method to the present analyses for consistency.

3. Assignment of each layer line to an inner or outer tube

A pair of chiral angles measured on a single DWNT is attributed to either an inner or an outer tube by examining the intensity modulations of layer lines. An enlarged ED pattern around a pair of (10) layer lines in Fig. 1 is shown in Fig. 3(a). The part of the layer line indicated by a pair of

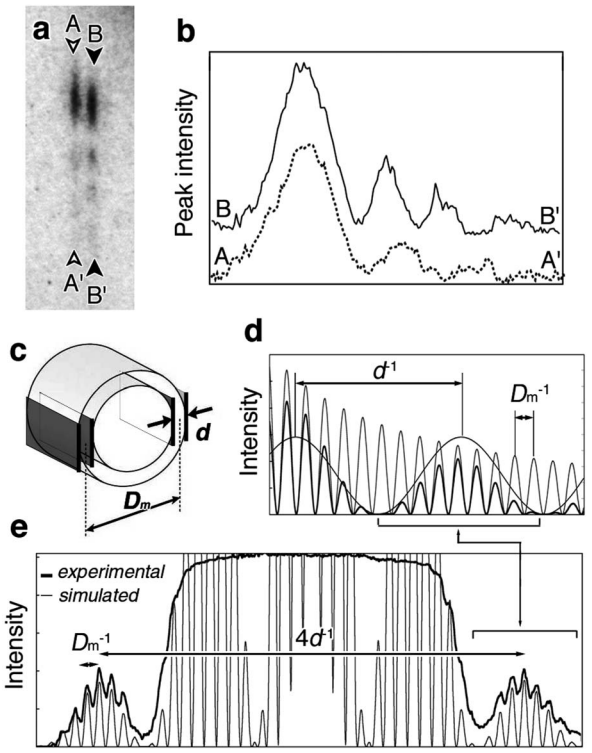

FIG. 3. (a) Enlargement of a pair of layer lines in Fig. 1(b). (b) Diffraction intensity profiles of the layer lines shown by open and solid arrowheads in (a), obtained along A-A' and B-B', respectively. (c) Definitions of interlayer distance (d) and mean diameter (D_m) of a DWNT. The diffraction intensity of the equatorial line is approximately described by the product of two oscillations related to D_m and d. (d) Line graphs of $f(k)=|J_0(2\pi D_m k)|^2$, $g(k)=|\cos(2\pi dk)|^2$, and their product (bold line). (e) Experimental and simulated intensity profiles of the equatorial line for the ED pattern in Fig. 1(b). The simulated profile fits the experimental one when the values of D_m and d are 3.05 and 0.35 nm, respectively.

open arrowheads corresponds to a corner of the hexagon shown by a dotted line, and the layer line marked by a pair of solid arrowheads corresponds to a corner of the hexagon with a solid line in Fig. 1(b). Diffraction intensity profiles of these two layer lines traced along A-A' and B-B' are shown in Fig. 3(b). The diffraction intensity along a layer line is described by the nth-order Bessel function, where n depends directly on the chiral indices of the SWNT.[13,19,20] The intensity modulations suggest the presence of pseudo-oscillations, which have an asymptotic period inversely proportional to the tube diameter. Therefore, the diameter of each tube can be determined from these periodicities, as will be shown in Sec. II C 4.

In Fig. 3, the oscillation period of the layer line marked with open arrowheads in Fig. 3(a) is longer than that of the one denoted by solid arrowheads, which can be seen more clearly in Fig. 3(b). The difference directly suggests that the open-arrowed layer lines [see hexagon denoted by the dotted line in Fig. 1(b)] are from the inner tube and the solid-arrowed ones (hexagon denoted by the solid line) are from the outer tube.

If the diffraction intensities are insufficient for examining the details of layer lines, we employ an alternative way to examine a relative difference between the diffraction intensities of the two types of layer lines.[21] This difference originates in the number of atoms contributing to the ED. The number of carbon atoms comprising a nanotube of a given length is proportional to the tube diameter, so that the diffraction intensity of the inner tube should be weaker than that of the outer tube. For the sake of clarity, we examined the diffraction intensities by integrating over the first peak of the intensity profile as shown in Fig. 3(b). Furthermore, the intensities of all (10) diffraction rods (spots) in Fig. 1(b) were measured, except for the overlapped ones, and the average intensity ratio of solid-arrowed rods to open ones was found to be about 1.3. On the other hand, the diameter ratio between inner and outer tubes for this particular DWNT (D_o/D_i), which was roughly estimated from its HRTEM image, was 1.26. This is close to the intensity ratio estimated from the diffraction profiles. Accordingly, we conclude that the layer line indicated by the solid arrowheads corresponds to the diffraction from the outer tube, and the other layer line indicated by the open arrowheads corresponds to the inner tube.

4. Measurement of tube diameter

The diameter of a nanotube can be examined using the pseudoperiods of layer lines as stated in the previous section. This procedure is, however, not always applicable; some tubes are not suitable for highly accurate measurement of the oscillation in layer lines due to some experimental constraints. For example, some tubes were too small to measure the layer lines with a desirable signal to noise (SN) ratio. In this case, the equatorial line was examined to obtain the tube diameters instead, since the SN ratio of this line is much higher than that of the other layer lines. As a very good approximation,[13] the equatorial line can be regarded as the ED pattern of a continuum cylinder. Therefore, a DWNT is represented by a convolution of a continuum cylinder D_m in diameter and a double slit with a separation d, where D_m corresponds to the mean diameter of the DWNT (average of diameters of inner and outer tubes), and d to the separation between the two layers [Fig. 3(c)].[22] Accordingly, the oscillating behavior of the equatorial line is described by the product of two types of oscillations with periods D_m^{-1} and d^{-1} [Fig. 3(d)]. The diffraction intensity profile along the equatorial line in Fig. 1(b) is shown by a bold line in Fig. 3(e). The measured values of D_m and d in Fig. 1 were 3.25 ± 0.2 nm and 0.36 ± 0.02 nm, respectively. Inner and outer tube diameters (D_i and D_o, respectively) can be calculated by using the relationships $D_i=D_m-d$ and $D_o=D_m+d$. It is noted that these measured values still contains rather large errors, so that the accuracy will improve as described in Sec. II C 5 by repeating the comparison between the experimental diffraction pattern and the simulated ones.

The values of d, D, D_i, and D_o may also be measured on the HRTEM images. However, nanotubes often vibrate during this observation due to thermal instability or charge-up disturbance of the specimen support grid. Such vibrations become an obstacle to the recording of HRTEM images with high resolution. In addition, it is noted that the values measured directly from HRTEM images should carry systematic

errors due to the curvature of the nanotubes. In HRTEM imaging, any objects with a spherical shell structure or a cylindrical structure give a smaller value for the diameter than the real one. Normally, the lattice image contrast from a crystal corresponds to the two-dimensional projection of the atomic density distribution (only when satisfying the Scherzer condition). In the case of a nanotube, the maximum peak of the atomic density on the projection is biased toward the inside of the diameter due to the tube curvature. It is also well known that the value of the diameter deduced from a HRTEM image changes critically depending on the imaging focus condition.[23] For example, according to Qin *et al.*, the measured diameter of a nanotube using the HRTEM image was 0.25–0.35 nm, but the simulation suggests the true value to be 0.4 nm.[24,25] Therefore, an accurate value of the tube diameter should be determined by using not only HRTEM imaging but also another method such as ED with its simulation. The curvature effect of HRTEM imaging has been nicely demonstrated in image simulation of nanotubes in Refs. 26 and 27.

5. Determination of chiral indices

From the experimentally measured values of D_m, d, and α_{exp} for the inner and outer tubes, and the deduced value of θ, we determined $(n_i,m_i)@(n_o,m_o)$. It should be noted that the measured values from the experimental ED pattern require careful comparison to the theoretical calculations. As mentioned above, the value of α_{exp} is not exactly equal to the true chiral angle (α), so that a correction must be taken into account. Furthermore, the tilt of the nanotubes against the incident beam should be also modified, as stated above. Here, simulations of the ED patterns for all (n,m) tubes $(0 \le m \le n < 70)$ were carried out, and we made a dataset of apparent chiral angles and diameters from ED patterns to compare with the true values defined by Eqs. (1) and (2). The simulated ED patterns of a nanotube were obtained by calculating the diffraction amplitude given on the basis of a first-order Born approximation, for all layers of the nanotube by taking account of the wavelength and incident direction of the electron beam. The program for the simulation of the ED pattern was courtesy of the DIFFRACT code[13] presented by Lambin.[15–17]

The procedure for determining the chiral indices is as follows. First, we find all candidates for chiral indices of a DWNT satisfying all values measured within the experimental error range. The ED pattern of each candidate is simulated and compared with the experimental pattern. For comparison, the diffraction intensity on the equatorial line is first examined, because this portion is not affected by the tilt of the nanotube. By using the equatorial line, a simulated ED pattern is calibrated. We selected the candidate for chiral indices, since the equatorial line exactly corresponds to the experimental pattern. That is, the values of D_m and d can be refined. Then, the positions and intensities of the simulated layer lines are compared with those in the experimental pattern. If the simulated pattern does not exactly correspond to the experimental pattern, the tilt angle is rededuced based on the difference in both patterns, and the value of the chiral angle is modified. The ED pattern is then simulated again on the basis of the modified values, and compared to the experimental pattern. By repeating these modification processes until the simulated and experimental ED patterns match well, this procedure enables us to determine the chiral indices with quite high accuracy.

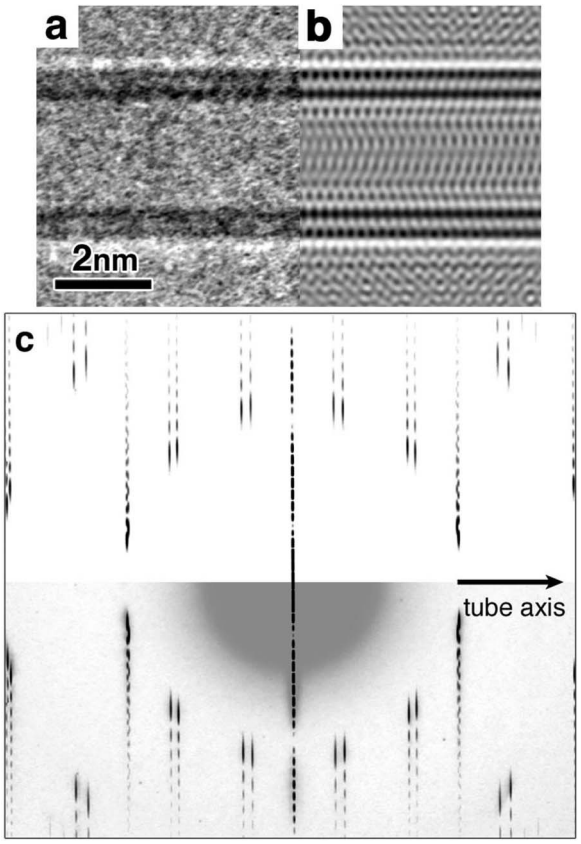

FIG. 4. Experimental (a) and simulated (b) HRTEM images of a $(28,11)@(37,11)$ DWNT, where the simulation was carried out by using the multislice method with a spherical aberration coefficient $C_s=1.2$ mm and defocus $\Delta f=68$ nm. Part of the simulated ED pattern of $(28,11)@(37,11)$ with a tilt angle of 2° is in (c) and (d).

In the case of the DWNT shown in Fig. 1, only one of the chiral indices candidates finally corresponds to the ED pattern, and the indices were determined to be $(28,11)@(37,11)$. This indicates that the analytical procedure for an ED pattern in this experiment has a high enough accuracy to uniquely determine the chiral indices. For reference, a simulated TEM image and a simulated ED pattern of $(28,11)@(37,11)$ are shown in Fig. 4, respectively, and they well consist with observed results of Fig. 1.

Although the analysis of ED pattern with four sets of layer lines was demonstrated above, three sets of layer lines can be found in several ED patterns as shown in Fig. 5(b), which occurs when one tube in the DWNT has an achiral structure and the other has a chiral one. Such an ED pattern can be analyzed in the same way as for the four sets of layer lines. The chiral indices of the DWNT recorded in Fig. 5(b) were determined to be $(15,15)@(30,9)$.

III. RESULTS

Three typical HRTEM images of DWNTs are shown in Fig. 6. The dark objects are catalytic metal particles, which

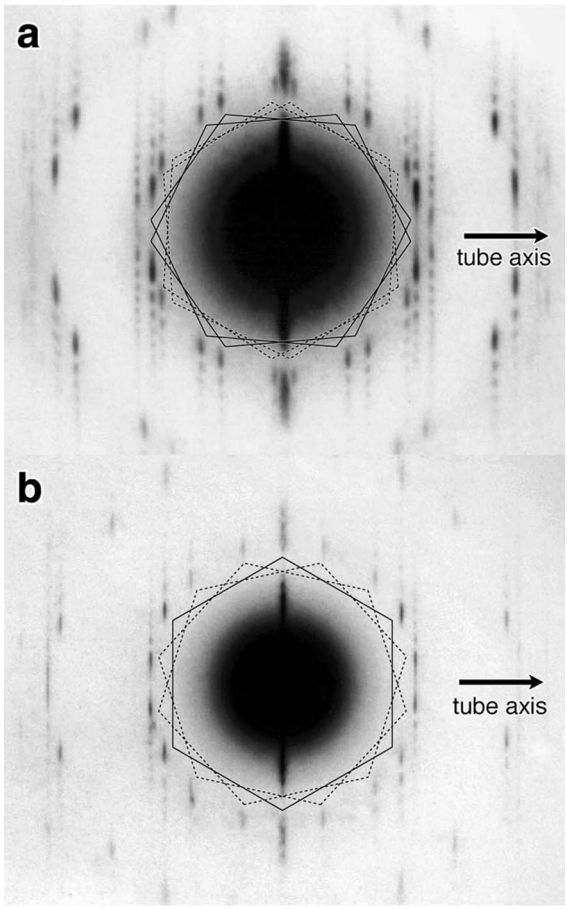

FIG. 5. ED patterns of DWNTs. The set of chiral indices for the DWNT shown in (a) is represented by $(20,15)@(33,11)$. In (b), three sets of layer lines can be seen, since one pair of layer lines overlaps, where the layer lines exhibit an achiral-type nanotube. The set of chiral indices for (b) is determined as $(15,15)@(30,9)$.

are present in the specimen as well as the amorphous carbon. We confirmed that more than 95% of the carbon nanotubes found in the sample were DWNTs. These DWNTs have diameters of 2–6 nm.

Various orientations of the hexagonally arranged ED patterns of DWNTs were observed and typical examples are shown in Fig. 5. It is obvious that the DWNTs grew with various chiral structures. About 90% of the DWNTs showed four sets of layer lines as shown in Fig. 5(a), while the remaining DWNTs showed three sets of layer lines as in the ED pattern of Fig. 5(b). No ED patterns showed only one or two sets of layer lines. It means that all the DWNTs examined in the present experiment do not have correlation in chiral angles between their inner and outer tubes.

In the present experiment, we determined carefully chiral indices of 141 randomly chosen isolated DWNTs. The distribution of the chiral indices of the DWNTs is visualized in Fig. 7. The positions of identical numbers in the two chiral maps of Figs. 7(a) and 7(b) represent the pair of chiral indices for the inner and outer tubes of the same DWNT. For example, the DWNT numbered 1 in both figures is $(13,6)@(24,3)$. Chiral indices of both the inner and outer tubes are mapped in Fig. 7(c). The map proves that the

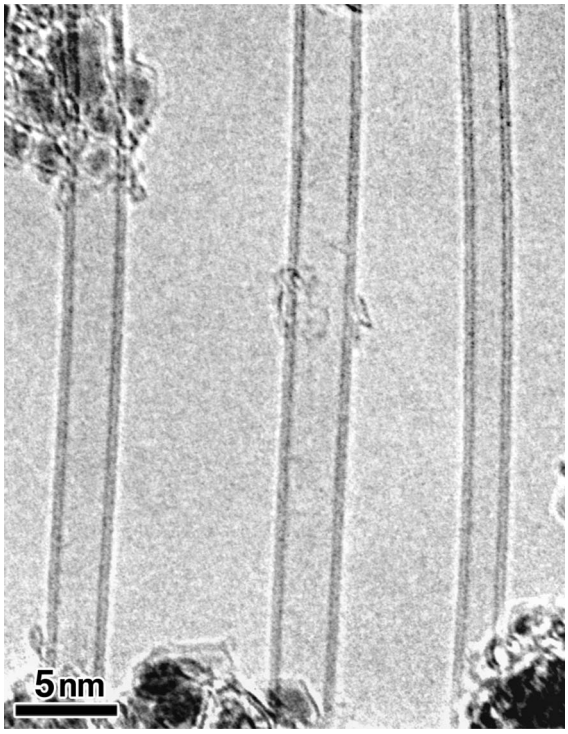

FIG. 6. HRTEM image of DWNTs prepared by arc discharge.

DWNTs examined in this experiment have a variety of chiral indices without any particular preference. However, the distribution of chiral indices appears to incline toward the small-diameter region ($D < \sim 3$ nm). In order to investigate a possible correlation in double-layer structures of the DWNTs, we analyzed statistical distributions on the diameters and chiral angles in the following section. It is noted that the values of the diameters and chiral angles used for the statistical analysis are the redefined values instead of the ones directly measured on ED patterns; they were corrected after calculating their chiral indices (n,m), according to Eqs. (1) and (2). Therefore, inevitable measurement errors arising from the HRTEM observations can be excluded.

IV. DISCUSSION

A. Diameter and interlayer distance of DWNTs

The diameter distributions are shown in Fig. 8(a), where the two bar charts and the line graph represent the distributions of D_o, D_i, and D_m, respectively. The figure shows that the tube diameters range mostly from 1.5 to 5.5 nm. The average value of D_m is 3.0 nm. Figure 8(b) shows the distribution of the interlayer distance of the DWNTs (d), where the values of d were obtained by $(D_o - D_i)/2$. It is of interest to point out that the interlayer distance distributes over a relatively wide range of 0.34–0.38 nm. The average value was 0.358 ± 0.001 nm. The value is 7% greater than that of bulk graphite (0.335 nm),[28] and about 5% greater than that of common MWNTs with several layers ($\sim$0.34 nm).[1,29] Therefore, we can say that this large interlayer distance originates from the small number of graphitic layers, which will

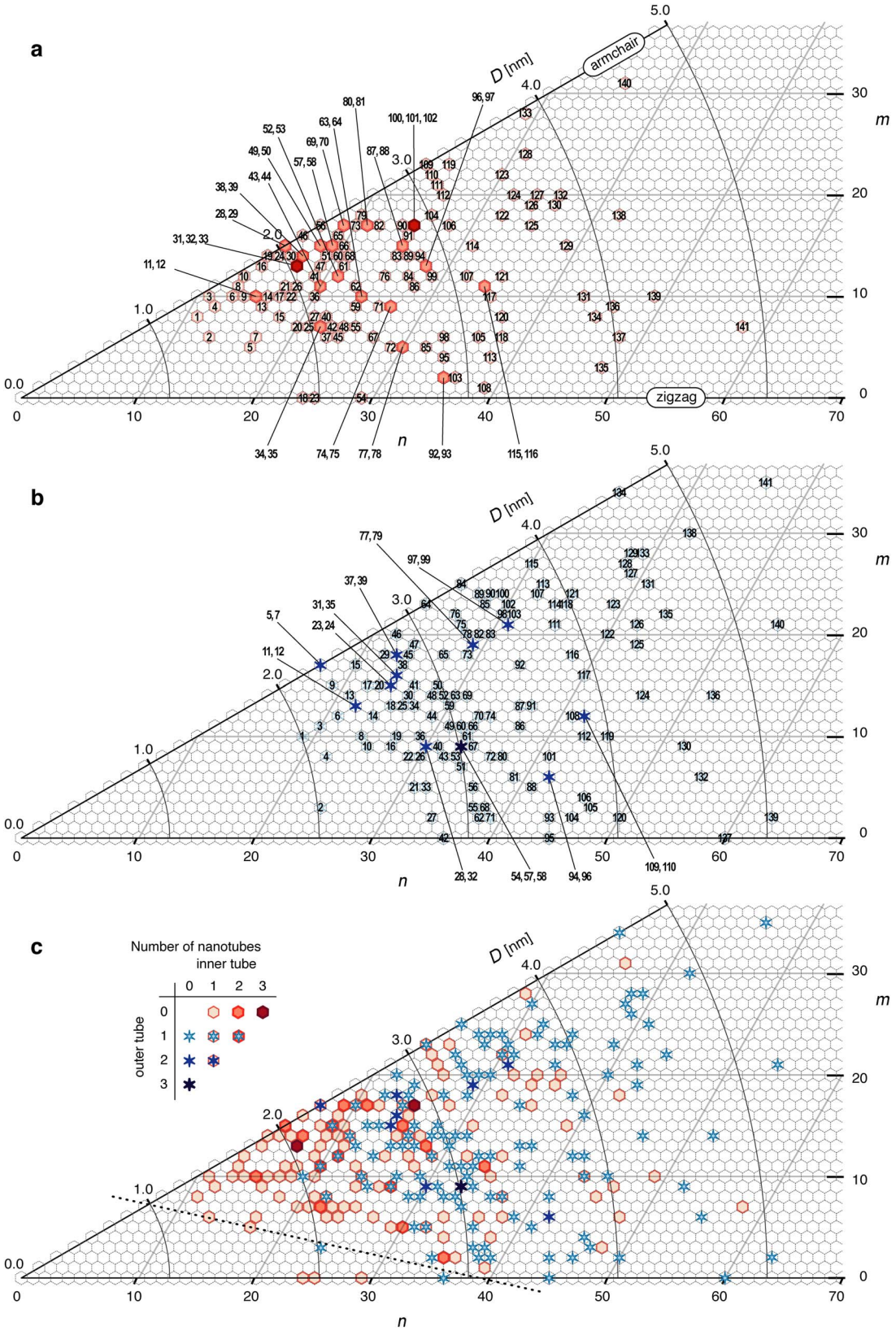

FIG. 7. (Color online) Distribution of chiral indices. Identical numbers on the two chiral maps in (a) and (b) indicate, respectively, the inner and outer tubes in the same DWNT, and the positions of the numbers represent the chiral indices. For example, the DWNT numbered by 1 is $(13,6)@(24,3)$. Chiral indices of both inner and outer tubes for all DWNTs examined are plotted in (c), where the inner and outer tubes and their numbers are denoted by marks in the inserted matrix. The chiral vectors are indicated by $\boldsymbol{a}_1$ and $\boldsymbol{a}_2$ in (a). Here, please note that the directions of these chiral vectors are different from those of the hexagonal lattice vectors used in the analyses of ED pattern.

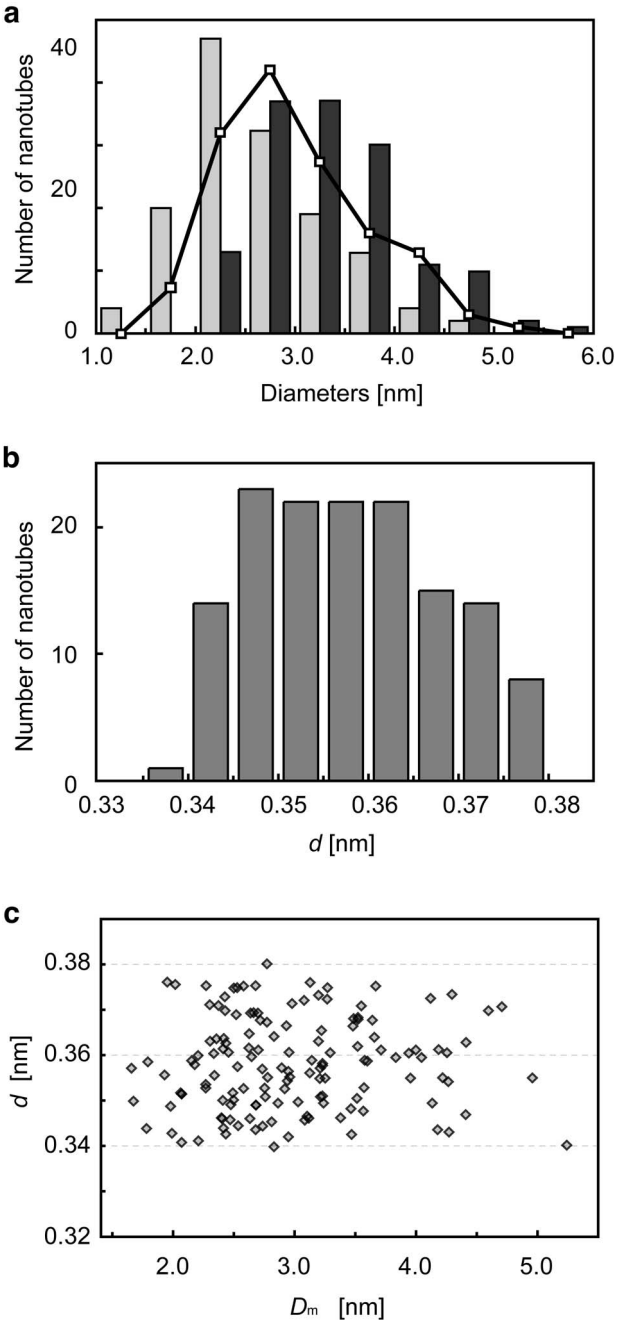

FIG. 8. Distributions of tube diameters and interlayer distance, and mean diameter dependence on interlayer distance. Distributions of the tube diameters are demonstrated in (a). The two bar charts correspond to those for the outer and inner tubes (D_o and D_i) and the solid line is for the mean diameter (D_m). The distribution of interlayer distance (d) is given in (b). The values of d are distributed over a relatively wide range (0.34–0.38 nm) with the average of 0.358 ± 0.001 nm. The correlation between d and D_m of individual DWNTs is given in (c).

be discussed later. In addition, this anomaly in the interlayer distance is consistent with other experimental results obtained by using Raman scattering[30] and x-ray diffraction.[31]

Next, we examined a relationship between the interlayer distance and the tube diameter. Correlation between d and D_m for individual DWNTs examined here is rather scattered as shown in Fig. 8(c), namely, it indicates that the anomaly in the interlayer distance should occur irrespective of the tube diameter.[32]

The large interlayer distance observed here is similar to that reported for a pair of large planar graphene sheets.[33] We also confirmed that such a large interlayer distance has been found in another type of DWNTs; these were prepared from C_{60}-encapsulating SWNTs with an outer diameter of about 1.4 nm,[30,34] which is much smaller than the present DWNTs. Accordingly, we propose that the expansion of the interlayer distance found for DWNTs may not originate from the curvature of the graphitic layer, but rather from the number of layers constituting the tube. To verify this proposal, we examined the interlayer distances of triple-wall nanotubes (TWNTs). Although only a few samples were examined, the mean interlayer distance of TWNTs with D values of 3–4 nm was found to be about 0.35 nm. This value is about 4% greater than that of MWNTs and about 2% smaller than that of DWNTs. For MWNTs with more than 10 layers, the interlayer distance was about 0.34 nm. These results also suggest that the anomaly in the interlayer spacing depends on the number of graphitic layers of nanotubes.

B. Chirality of DWNTs

The chiral indices examined in this study tend to be distributed in the region above the dotted line drawn in Fig. 7(c). This suggests that the range of the chiral angle distribution changes depending on the tube diameter. The angles of the larger diameter nanotubes (>3 nm) were distributed more widely, covering randomly the chiral map.[35] To clarify such tendency, we took chiral angle distributions separately from the regions with different tube diameters. Figure 9(a) shows the chiral angle distributions of inner and outer tubes with diameters smaller than 3 nm. It indicates that both inner and outer tubes have a tendency to approach the chiral angles to be 30°; more than half of the tubes have the chiral angles in the range between 20 and 30°. In contrast, the chiral angle distributions for both inner and outer tubes with diameters larger than 3 nm have no tendency as shown in Fig. 9(b). Therefore, we can conclude with confidence that the chiral angle distribution depends on the tube diameter.

We examined whether or not there are any preferred combinations of the chiral angles between inner and outer tubes. Apparent differences in the chiral angles between inner and outer tubes examined for individual DWNTs ($\Delta\alpha$) are shown as the bar chart in Fig. 10. Here, $\Delta\alpha$ is equal to the difference between the absolute values of two α, i.e., $||\alpha_{\text{inner}}|-|\alpha_{\text{outer}}||$ (for example, even if $\Delta\alpha$ for a DWNT is equal to 0°, two types of correlations can be considered, namely, either 0° or 2α). In order to find distinct features for the distribution of $\Delta\alpha$ obtained in the present experiment, the probability distribution of $\Delta\alpha$ for all $(n_i,m_i)@(n_o,m_o)$ in the ranges $1.5 < D_m < 6$ nm and $0.34 < d < 0.38$ nm was calculated as reference data. The result is shown by the solid line in Fig. 10. The experimental distribution of $\Delta\alpha$ and the reference data agree well with the reliability of 95%. Therefore, it can be concluded that the correlation on the orientations of the hexagonal carbon network between the inner and outer tubes is independent.

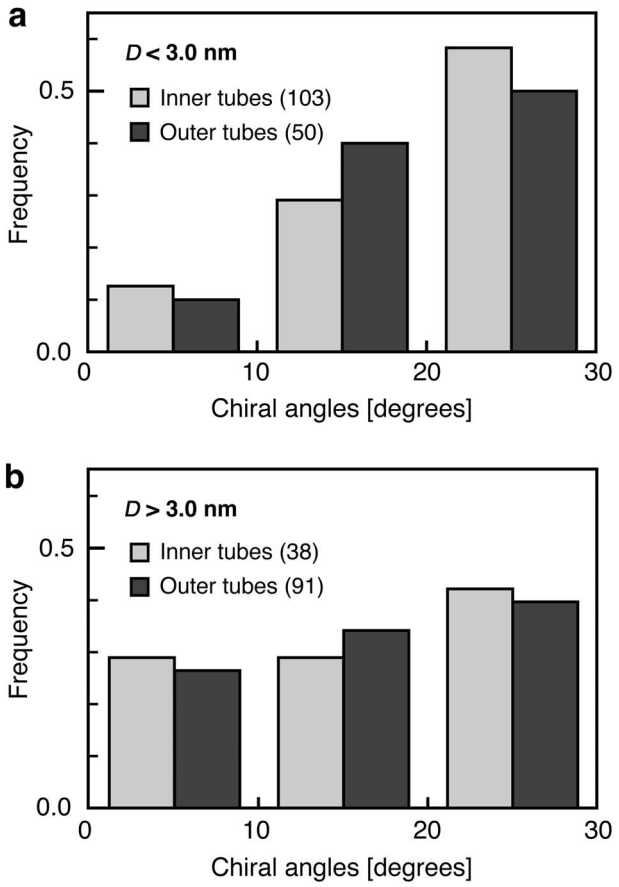

FIG. 9. Distributions of the chiral angles of inner and outer tubes with diameters less than 3 (a) and more than (b) 3 nm. Numbers in parentheses indicate the total numbers of nanotubes.

We now consider the random orientation of the graphitic layers observed in inner and outer tubes of DWNTs. Generally, it has been said that the geometrical structure of a MWNT follows a stacking rule; the interlayer distance of the MWNT will be adjusted to minimize the total energy of the system. This allows a few limited candidates of chiral indices with appropriate tube diameters for making individual layers, so that MWNTs, especially with small diameters, should require a turbostratic structure as reported in Ref. 5. Under such limited conditions, DWNTs examined in the present study, however, have sufficiently large diameters ($D > \sim 2$ nm). This condition allows too many candidates to be selected for chiral indices, so the above restriction is no longer applicable. Therefore, if any matching of the chiralities between the inner and outer tubes of a DWNT takes place during the layer growth, such predispositions may appear in the experimental data. The results obtained in this study, however, did not show any peculiar tendency for $\Delta\alpha$. This indicates that the random orientation of the graphitic layers in the inner and outer tubes of a DWNT is accompanied not only by the geometrical restriction proposed in Ref. 5 but also by the energetic stability.

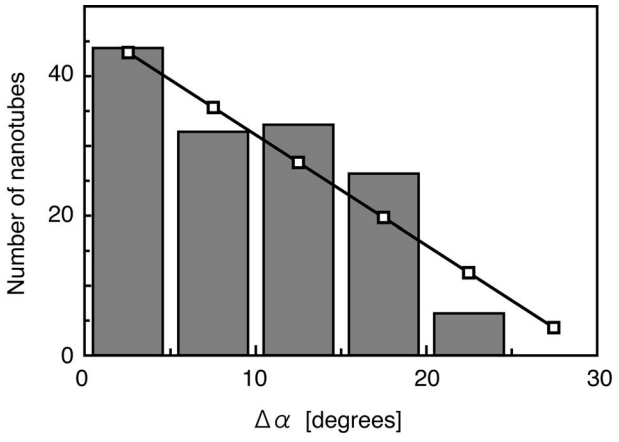

FIG. 10. Distribution of the difference in the chiral angles ($\Delta\alpha$) between inner and outer tubes of individual DWNTs. The experimental data are shown as a bar chart, and a reference distribution, which is obtained by calculating $\Delta\alpha$ for all (n_i,m_i) @ (n_o,m_o) in the ranges $1.5 < D_m < 6$ nm and $0.34 < d < 0.38$ nm, is shown as a line graph.

TABLE I. Number (and percentage) of metallic and semiconducting nanotubes estimated for inner and outer tubes of individual DWNTs.

	Outer tube		
Inner tube	Metallic	Semiconducting	Total (%)
Metallic	25	33	58 (41)
Semiconducting	34	49	83 (59)
Total (%)	59 (42)	82 (58)	141 (100)

Metallic or semiconducting behavior

All nanotubes observed in this study should be classified into either metallic or semiconducting, by taking into account of the chiral indices determined above (Fig. 7). According to the theoretical arguments, the electronic properties of a carbon nanotube are related to its chiral index, which results in one-third of conceivable nanotubes exhibiting metallic behavior and the remaining two-thirds exhibiting semiconducting one.[36,37] Table I summarizes the numbers of metallic and semiconducting nanotubes found for the inner and outer tubes examined here, and their combinations. As a result, 41–42 % of both inner and outer tubes are classified as metallic. This ratio is significantly higher than the expected value ($1/3 \approx 33\%$) with the reliability of 95%. Furthermore, as explained in Fig. 7, the chiral angles tended to dominate 30° when the tube diameters become smaller than 3 nm. Since the armchair tubes have all metallic character, it is expected to dominate the metallic ratio greater for small diameter tubes. With such an expectation, we checked the metallic ratios in the two cases: one is for the tubes with diameter smaller than 3 nm and the other is greater than 3 nm. The results indicated, respectively, 43% and 39%. It seems that the metallic character dominated in the tubes with small diameters, but the difference is only 4% which is almost within the error. Therefore, we conclude that the metallic

ratio is slightly greater for all the tubes measured, and this result suggests that the possibility of some rule for selective growth of metallic nanotubes under the growth condition employed in the present experiment. In addition, no significant selectivity was recognized in the combination of metallic and semiconducting nanotubes found in the inner and outer tubes of individual DWNTs.

V. SUMMARY

Chiral indices of individual DWNTs prepared by arc discharge method were uniquely determined by examining ED, and the structural correlation between two adjacent layers (namely, the inner and outer tubes) of the DWNTs was studied based on statistical analysis. An anomaly in the interlayer distance was observed between inner and outer tubes. The interlayer distances were in the range of 0.34–0.38 nm, with an average of 0.358 ± 0.001 nm. The value was about 7% larger than that for graphite. The large interlayer distance was not related to the tube diameter, but rather to the number of layers constituting the nanotubes.

Both inner and outer tubes indicated a tendency to distribute toward higher chiral angles (approaching 30°) when the tube diameters were smaller than 3 nm. In particular, more than half of such small diameter nanotubes have chiral angles in the range of 20–30°. For tubes with large diameters (>3 nm), the chiral angles were distributed over whole the chiral map (0–30°). The orientation of the hexagonal network structure did not show any significant correlation between the inner and outer tubes, suggesting that the orientation did not have much effect on stabilizing the DWNTs.

More than 40% of all nanotubes observed in this study was classified as metallic. This ratio is significantly higher than the expected value. In addition, there was no selective combination of metallic and semiconducting nanotubes between inner and outer tubes.

ACKNOWLEDGMENTS

M. K. thanks L. Henrard and Ph. Lambin for providing the FORTRAN code DIFFRACT. S. B. acknowledges the Grant-in-Aid for Scientific Research (C), No. 16510092, from the Ministry of Education, Culture, Sports, Science and Technology of Japan. This work was supported by the U.S. Office of Naval Research (Grant No. ONR-N000140010762) and the Japan Science and Technology Agency.

*Corresponding author. Present address: Division of Nanomaterials Science, Eco Topia Science institute, Nagoya University, Furo-cho, Chikusa-ku, Nagoya 464-8603, Japan. Email address: hirahara@esi.nagoya-u.ac.jp

[1] S. Iijima *et al.*, Mater. Sci. Eng., B **19**, 172 (1993).
[2] T. Guo, P. Nikolaev, A. G. Rinzler, D. Tománek, D. T. Colbert, and R. E. Smalley, J. Phys. Chem. **99**, 10694 (1995).
[3] S. Iijima, Nature (London) **354**, 56 (1991).
[4] L. C. Qin, T. Ichihashi, and S. Iijima, Ultramicroscopy **67**, 181 (1997).
[5] X. F. Zhang, X. B. Zhang, G. Van Tendeloo, S. Amelinckx, M. Op de Beeck, and J. Van Landuyt, J. Cryst. Growth **130**, 368 (1993).
[6] S. Iijima and T. Ichihashi, Nature (London) **363**, 603 (1993).
[7] L.-C. Qin, in *Progress in Transmission Electron Microscopy 2, Applications in Materials Science*, Springer Series in Surface Sciences, Vol. 39 (Springer-Verlag/TUP, Berlin, 2001), p. 73.
[8] S. Roche, F. Triozon, A. Rubio, and D. Mayou, Phys. Rev. B **64**, 121401(R) (2001).
[9] R. Saito, R. Saito, R. Matsuo, T. Kimura, G. Dresselhaus, and M. S. Dresselhaus, Chem. Phys. Lett. **348**, 187 (2001).
[10] M. Gao, J. M. Zuo, R. D. Twesten, I. Petrov, L. A. Nagahara, and R. Zhang, Appl. Phys. Lett. **82**, 2703 (2003).
[11] J. C. Meyer, M. Paillet, T. Michel, A. Moréac, A. Neumann, G. S. Duesberg, S. Roth, and J.-L. Sauvajol, Phys. Rev. Lett. **95**, 217401 (2005).
[12] M. S. Dresselhaus, G. Dresselhaus, and P. C. Eklund, *Science of Fullerenes and Carbon Nanotubes* (Academic Press, San Diego, 1996), p. 11.
[13] Ph. Lambin and A. A. Lucas, Phys. Rev. B **56**, 3571 (1997).
[14] Here it is noted that we use the two-dimensional Miller index (*hk*) instead of three-dimensional index (*hki*0), since a single graphene sheet is simply regarded as a two-dimensional hexagonal lattice.
[15] M. Kociak, K. Hirahara, K. Suenaga, and S. Iijima, Eur. Phys. J. B, **32**, 457 (2003).
[16] M. Kociak, K. Suenaga, K. Hirahara, Y. Saito, T. Nakahira, and S. Iijima, Phys. Rev. Lett. **89**, 155501 (2002).
[17] K. Hirahara, S. Bandow, H. Kataura, M. Kociak, and S. Iijima, Phys. Rev. B **70**, 205422 (2004).
[18] The reading error is related to the value of the apparent angle against the tube axis. For example, the magnitude of the reading error in 2β is estimated to be $\sim 0.2°$ when $\beta < 5°$, and to be $\sim 0.5°$ when $\beta > 5°$, when a tube lies tilted by 15° against the incident electron beam.
[19] Z. Liu and L.-C. Qin, Chem. Phys. Lett. **400**, 430 (2004).
[20] L. Henrard, A. Loiseau, C. Journet, and P. Bernier, Eur. Phys. J. B **10**, 263 (1999).
[21] The comparison of diffraction intensities is useful under a specific condition: two layer lines on the ED pattern should appear close to each other as in Fig. 1(b), because the diffraction intensity along a layer line is affected by tan α_{exp}.
[22] Another useful approximation is to consider that the diffraction occurs predominantly in the portion where the walls of the DWNT are parallel to the incident electron beam [shaded regions in Fig. 3(c)]. Then the scattering centers are approximately represented by the convolution of two sets of parallel slits with the different separations D_{m} and d.
[23] N. Wang, in *Electron Microscopy of Nanotubes*, edited by L. Wang and C. Hui (Kluwer Academic, MA, 2003), Chap. 4.
[24] L.-C. Qin, X. Zhao, K. Hirahara, Y. Miyamoto, Y. Ando, and S. Iijima, Nature (London) **408**, 50 (2000).
[25] L.-C. Qin, X. Zhao, K. Hirahara, Y. Ando, and S. Iijima, Chem. Phys. Lett. **349**, 389 (2001).

[26] C. Qin and L.-M. Peng, Phys. Rev. B **65**, 155431 (2002).
[27] S. Wang and D. Zhou, Chem. Phys. Lett. **225**, 165 (1994).
[28] R. Bacon, J. Appl. Phys. **31**, 284 (1960).
[29] Z. G. Li, Paul J. Fagan, and L. Liang, Chem. Phys. Lett. **207**, 148 (1993).
[30] S. Bandow, M. Takizawa, K. Hirahara, M. Yudasaka, and S. Iijima, Chem. Phys. Lett. **337**, 48 (2001).
[31] M. Abe, H. Kataura, H. Kira, T. Kodama, S. Suzuki, Y. Achiba, K. I. Kato, M. Takata, A. Fujiwara, K. Matsuda, and Y. Maniwa, Phys. Rev. B **68**, 041405(R) (2003).
[32] The correlation coefficient between d and D_m was calculated to be 0.038. The value is much smaller than the acceptable value for a linear regression with 70 degrees of freedom at a 5% significance level (0.232), suggesting that there is no significant correlation between d and D_m.
[33] S. Iijima *et al.*, Chem. Scr. **14**, 117 (1978-1979).
[34] K. Hirahara, S. Bandow, K. Suenaga, H. Kato, T. Okazaki, H. Shinohara, and S. Iijima, Phys. Rev. B **64**, 115420 (2001).
[35] The chirality distribution was discussed with respect to the absolute value of the chiral angle, since we could not adequately distinguish right- or left-handed chirality from the experiment.
[36] M. S. Dresselhaus, G. Dresselhaus, and P. C. Eklund, *Science of Fullerenes and Carbon Nanotubes* (Ref. 12), p. 809.
[37] R. Saito, G. Dresselhaus, M. S. Dresselhaus, *Physical Properties of Carbon Nanotubes* (Imperial College Press, London, 1998), p. 61.